Implementation of SENSE and Gradient Nonlinearity Correction in Continuously Moving Table MRI

H. H. Hu[1], A. J. Madhuranthakam[1], D. G. Kruger[1], J. F. Glockner[1], S. J. Riederer[1]
[1]Dept. of Radiology, Mayo Clinic College of Medicine, Rochester, Minnesota, United States

Introduction

The integration of SENSE with continuously moving table (CMT) MRI has previously been demonstrated [1,2]. The implementation of SENSE-CMT is not trivial, and must address specific issues including coils, sensitivity maps, and image reconstruction. Another issue is gradient warp (GW) or nonlinearity. Although GW effects have been identified and accounted for in non-SENSE CMT [3], the incorporation of GW correction with SENSE-CMT is not straightforward. Specifically, the GW phenomenon imposes constraints on the manner and order in which SENSE unfolding and GW correction must occur in CMT reconstruction. In the current work, we identify challenges in SENSE-CMT with GW, propose a correction algorithm, and present results from phantoms and peripheral CE-MRA exams.

Methods

GW effects manifest as positional distortions in image space and worsen with increasing FOV. In Fig.1a, GW contours are illustrated for a fixed FOV. The gray box represents a particular pixel that experiences a single level of GW distortion, the degree of which is determined by the relative location of the pixel from isocenter. In Fig.1b, GW effects in CMT for the case with readout along the axis of table motion [4], are illustrated. Three separate time points t_1, t_2, and t_3 are shown during table motion. For illustration simplicity, the table translates exactly one pixel along X (Δx) between adjacent time points. FOV_S is the actively-sampled sub-FOV that continuously interrogates the imaging volume. Note in particular that the same gray pixel experiences a different level of GW at each time point as a result of table motion. As FOV_S moves along X, the longitudinal and lateral locations of the pixel change with time. Therefore, the net GW effect experienced by this pixel is the sum of individual effects experienced at times t_1, t_2, and t_3 while the pixel remained in the moving FOV_S, and is distinctly different from that experienced in the fixed FOV scenario described in (a). Consequently, every pixel along the extended axis undergoes a spectrum of GW in CMT that leads to image blurring if not corrected.

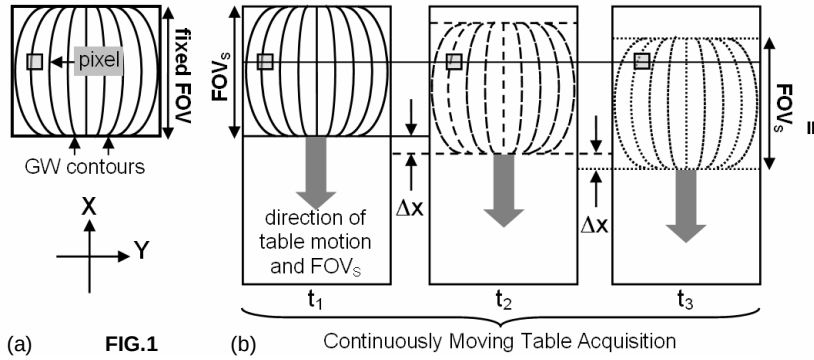

(a) **FIG.1** (b)

• *GW Correction in Non-SENSE CMT*

A GW correction algorithm for CMT was recently introduced [3]. In principle, the correction requires a separate 3D unwarping calculation for each phase encode, since each view is acquired at a distinct table location along X. In practice, the error level is tolerable if GW correction is performed on a small group of views (G=16-128) at a time. This reasoning assumes that the distance of table travel during a group of consecutively sampled views is short (1-8 pixels), within which the differential rate of GW errors is small. As a result, GW-corrected sub-images corresponding to separate view-groups are summed to yield the extended image.

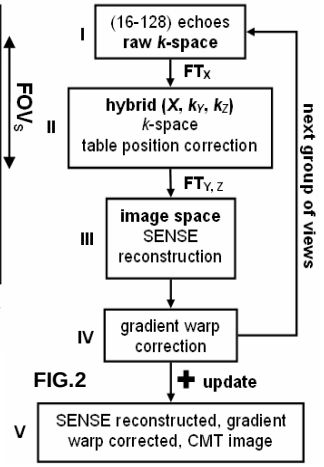

FIG.2

• *GW Correction in SENSE-CMT*

A concern in SENSE-CMT is that SENSE unfolding can be problematic if GW distortions cause significant spatial misregistration between coil calibration and accelerated data sets. Since SENSE unfolding and GW correction both operate in image space, the former must *precede* the latter in a SENSE-CMT reconstruction. However, the fact that GW correction operates on partial view-groups limits the SENSE unfolding process in CMT. As outlined in Fig.2, SENSE unfolding must also function on sub-images corresponding to small view-groups (III), and is subsequently followed by GW correction (IV). These steps are embedded in a loop that progressively sums reconstructed and unwarped sub-images (V). Blocks (I-II) are responsible for proper echo placement in CMT, and are described in detail in Ref. 4.

Results

The algorithm in Fig.2 was tested on a fixed-FOV phantom and CMT volunteer CE-MRA data acquired with a 1.5 Tesla GE Signa LX scanner. Fig.3 shows MIP images from a stationary resolution phantom and contrast-filled rods, acquired with a large 40 cm FOV and a 256×128×8 matrix. Since a fixed-FOV was used, table position correction (block II) was not performed. Fig.3a illustrates a non-accelerated image *without* GW correction. Note that the straight rods are warped at the edges of the FOV (arrowheads). Fig.3b shows the result after two-fold (Y-L/R) acceleration *with* SENSE and GW correction. A group size of G=16 views was used, thus looping through the algorithm 64 times (1,024 views total) to yield 64 separate unfolded and unwarped images. The accumulative sum of these 64 sub-images gives the result in Fig.3b. Note improved lateral resolution with SENSE (inserts), and the repositioning of the rods to their correct locations in the FOV.

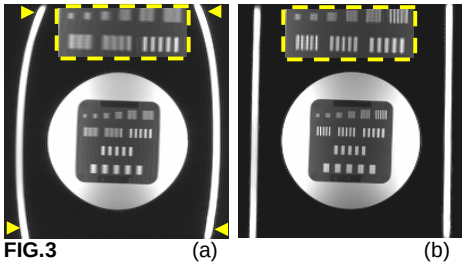

FIG.3 (a) (b)

Fig.4a shows a 90 cm mask-subtracted CMT peripheral angiogram acquired with an 8-element coil array and two-fold L/R SENSE after intravenous infusion of 20 mL of Gd-contrast. FOV_S was 25 cm with a 256×128×16 matrix. Reconstruction was performed with G=128 for 8,320 views. Fig.4 (b) and (c) show enlargements of the right femoral artery, without and with GW correction, respectively. Note improved visualization of branch vessels with GW correction (arrowheads).

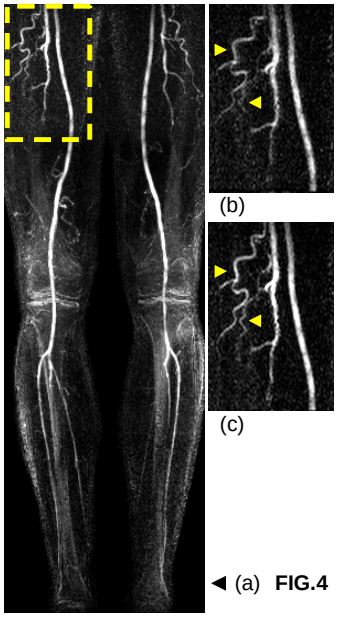

◀ (a) **FIG.4**

Conclusion

We have successfully demonstrated the manner in which GW correction can be incorporated into CMT MRI with SENSE.

References

[1] Keupp, et al. Proc. ISMRM 2004:324. **[2]** Hu, et al. Proc. ISMRM 2004:325. **[3]** Polzin, et al. MRM 2004; 52:181-187. **[4]** Kruger, et al. MRM 2002; 47:224-231.